# Silibinin Inhibits Established Prostate Tumor Growth, Progression, Invasion, and Metastasis and Suppresses Tumor Angiogenesis and Epithelial-Mesenchymal Transition in Transgenic Adenocarcinoma of the Mouse Prostate Model Mice

Rana P. Singh,[1,3] Komal Raina,[1] Girish Sharma,[1] and Rajesh Agarwal[1,2]

**Abstract**

**Purpose:** The chronic nature of prostate cancer growth and progression leading to metastasis provides a large window for intervention. Herein, for the first time, we investigated the effect and associated mechanisms of silibinin phosphatidylcholine (silybin-phytosome) on established prostate tumors in transgenic adenocarcinoma of the mouse prostate (TRAMP) model.

**Experimental Design:** Twenty-week-old TRAMP male mice having palpable prostate tumor were fed with control or 0.5% and 1%, w/w, silybin-phytosome diets for 11 weeks and then sacrificed.

**Results:** Dietary silibinin inhibited the growth of prostate tumors (up to 60%, $P < 0.001$) and suppressed tumor progression from prostatic intraepithelial neoplasia to differentiated adenocarcinoma and poorly differentiated adenocarcinoma, with a complete absence of poorly differentiated adenocarcinoma at higher doses. It also inhibited the incidence of tumor invasion of seminal vesicle (up to 81%, $P < 0.001$) with complete absence of distant metastasis. Silibinin moderately inhibited tumor cell proliferation and induced apoptosis, but strongly suppressed tumor microvessel density (up to 60%, $P < 0.001$), vascular endothelial growth factor, and vascular endothelial growth factor receptor-2 expression. Antibody array analysis of plasma showed a decrease in the circulatory levels of vascular endothelial growth factor and basic fibroblast growth factor. Decreased levels of matrix metalloproteinases (MMP), snail-1, and vimentin, and an increased level of E-cadherin were also observed, indicating the anti – epithelial-mesenchymal transition effect of silibinin in tumors.

**Conclusions:** Overall, silibinin treatment of TRAMP mice bearing prostate tumor inhibited tumor growth, progression, local invasion, and distant metastasis involving suppression of tumor angiogenesis and epithelial-mesenchymal transition. These findings would have greater relevance for the ongoing phase II clinical trial with silibinin-phytosome in prostate cancer patients.

The growth and progression of prostate cancer takes considerable amount of time that may range up to two to three decades from the time of initiation to the metastatic disease and thus provide a large window for different intervention strategies. In this regard, intervention of prostate cancer by nontoxic edible phytochemicals is an upcoming approach (1, 2). This treatment approach is advantageous for its lack of adverse health effect, its being economical, and its being acceptable for human oral consumption. Silibinin is a natural flavanolignan and has all these above characteristics, including its clinical use as an antihepatotoxic agent and dietary supplement as well as its anticancer activities in various models of epithelial cancers (2–4).

Prostate tumors are heterogeneous with regard to their cellular composition, development, molecular abnormalities, and clinical path (5). In the United States, although 1 in 6 men is diagnosed with prostate cancer, only 1 in 34 dies of the metastatic disease (6). In the beginning, prostate tumor growth is androgen dependent and treated with antiandrogen therapies; however, it progresses to a hormone refractory stage (7). At the advanced stages, molecular abnormalities are involved in enhancing the angiogenic, invasive, and metastatic capabilities in prostate cancer (8, 9). In this regard, prostate tumors show overexpression of vascular endothelial growth factor (VEGF) and VEGF receptor (VEGFR), leading to the receptor activation and downstream signaling to drive endothelial cell growth, proliferation, migration, and vessel organization (8). Tumors also express high levels of matrix metalloproteinases (MMP) that degrade tissue matrix and facilitate tumor as well as

**Authors' Affiliations:** [1]Department of Pharmaceutical Sciences, School of Pharmacy; [2]University of Colorado Cancer Center, University of Colorado Denver, Denver, Colorado; and [3]Cancer Biology Laboratory, School of Life Sciences, Jawaharlal Nehru University, New Delhi, India

Received 5/20/08; revised 7/1/08; accepted 7/10/08.

**Grant support:** National Cancer Institute RO1 grant CA102514.

The costs of publication of this article were defrayed in part by the payment of page charges. This article must therefore be hereby marked *advertisement* in accordance with 18 U.S.C. Section 1734 solely to indicate this fact.

**Requests for reprints:** Rajesh Agarwal, Department of Pharmaceutical Sciences, School of Pharmacy, University of Colorado Denver, 4200 East Ninth Street, Box C238, Denver, CO 80262. Phone: 303-315-1381; Fax: 303-315-6281; E-mail: Rajesh.Agarwal@uchsc.edu.

©2008 American Association for Cancer Research.

doi:10.1158/1078-0432.CCR-08-1309

Downloaded from http://aacrjournals.org/clincancerres/article-pdf/14/23/7773/1979631/7773.pdf by guest on 03 March 2024

## Translational Relevance

The relevance of this study is that silibinin is currently in clinical trials for prostate cancer and yet its antitumor effects and mechanisms are not completely understood. Herein, we observed that silibinin suppresses (*a*) tumor growth by 60%, (*b*) progression from prostatic intraepithelial neoplasia to adenocarcinoma (zero incidence of poorly differentiated adenocarcinoma at higher dose), (*c*) invasion of seminal vesicle by 80%, and (*d*) metastasis (zero incidence) in a preclinical transgenic mouse model of prostate cancer (TRAMP), which closely mimics the human prostate cancer progression. Specifically, the drug was administered to mice with palpable prostate tumors (at 20-week age), a similar situation with many clinical cases of human prostate cancer at the time of diagnosis. Antiproliferative, proapoptotic, antiangiogenic, and anti-invasive effects of silibinin satisfactorily accounted for why tumors remain smaller and did not invade the adjacent tissues and metastasize. Silibinin (*a*) reduced vascular endothelial growth factor and vascular endothelial growth factor receptor-2 expression in tumors, and circulating titer of vascular endothelial growth factor and basic fibroblast growth factor, and (*b*) altered the expression of matrix metalloproteinases as well as snail-1, vimentin, and E-cadherin to suppress epithelial-mesenchymal transition in tumors. Overall, these results are of clinical relevance and would provide impetus to widen the ongoing clinical trials for prostate cancer intervention with silibinin.

endothelial cell invasion and migration (9). Furthermore, epithelial-mesenchymal transition (EMT) has also been observed in epithelial tumor cells to facilitate these biological processes, in which tumor cells lose E-cadherin, a characteristic of epithelial cells, and express vimentin, a characteristic of mesenchymal cells (10, 11). This could be regulated by a transcription factor, called snail-1, which suppresses the expression of E-cadherin (10, 11). Therefore, antiangiogenic as well as anti-invasive strategies could be prospective and proficient approaches to intervene prostate cancer growth, invasion, and metastasis.

Silibinin has shown strong anticancer efficacy against both androgen-dependent and androgen-independent prostate cancer LNCaP, 22Rv1, PC-3, and DU145 cells (12–14). In prostate cancer cell culture studies, silibinin causes cell cycle arrest by modulating cyclin-dependent kinase (CDK)-cyclin-CDK inhibitor and retinoblastoma-E2F axes, and induces differentiation morphology and growth arrest (12–14). It also inhibits epidermal growth factor receptor and insulin-like growth factor (IGF) receptor I signaling in prostate cancer cells (15, 16). In animal studies, oral silibinin suppresses the growth of DU145 and PC-3 xenografts in nude mice (17, 18). Recently, we observed the chemopreventive efficacy of silibinin in the transgenic adenocarcinoma of the mouse prostate (TRAMP) model in which mice were treated with silibinin from 4 to 24 weeks of age (19). In this study, silibinin modulated CDK-cyclin-CDK inhibitor axis and IGF-receptor type Iβ signaling, without affecting the transgene expression, for its antitumor efficacy against the localized prostate tumor. However, the effects and associated mechanisms of silibinin on localized prostate tumor that follows the course of invasion and metastasis in TRAMP mice have not yet been studied.

In the present study, we evaluated the efficacy of silibinin phosphatidylcholine complex (silybin-phytosome) on established prostate tumor growth, progression, invasion, and distant metastasis in TRAMP mice. Additionally, we also investigated the biomarkers of antitumor effects and associated molecular mechanisms. The present findings revealed anti-invasive and antimetastatic activities of silibinin in this *in vivo* tumor model together with a strong antiangiogenic effect and inhibitory activity on EMT in silibinin-treated tumor tissues.

## Materials and Methods

***Animals and treatments.*** Heterozygous TRAMP females with C57BL/6 background were cross-bred with nontransgenic C57BL/6 breeder males. Genotyping was done by PCR-based screening assay for PB-Tag as reported (19), and routinely obtained TRAMP male mice were maintained on control diet for 20 wk. Mice were abdominally palpated for the presence of prostate tumors. Twenty-week-old TRAMP male mice, each having a palpable prostate tumor, were exposed to control AIN-93M diet ($n$ = 8 mice) or 0.5%, w/w, silibinin ($n$ = 8 mice) or 1%, w/w, silibinin ($n$ = 7 mice) in AIN-93M diet for 11 wk. The silibinin (Fig. 1A) used was silybin-phytosome, which is a commercial formulation (purchased from Indena Corporation) of the silibinin and phosphatidylcholine complex (~1:2 ratio by weight, respectively) and has shown better bioavailability of silibinin compared with the administration of pure silibinin (20). Ten 20-wk-old nontransgenic (C57BL/6) male mice were also fed with either control ($n$ = 5 mice) or 1%, w/w, silibinin diet for 11 wk. These diets were prepared commercially by Dyets, Inc. During the 11 wk of study, mice were permitted free access to drinking water and food and monitored for diet consumption, body weight, and general health. Animal care and treatments were in accordance with institutional guidelines and approved protocol.

***Histopathology.*** Animals were injected with heparin and euthanized by carbon dioxide asphyxiation. Blood was collected for harvesting plasma. At necropsy, animals were examined for gross pathology and any evidence of edema, abnormal organ size, or appearance in nontarget organs such as invasion of seminal vesicle and distant metastasis. Prostate along with seminal vesicles was removed en bloc and weighed. One portion of the prostate was snap frozen and stored at -80°C and the other was fixed overnight in 10% (v/v) phosphate-buffered formalin and processed conventionally. Liver, lung, kidney, lymph nodes (inguinal, cervical and mediastinal), and bone (femur) were also collected and fixed in formalin for histopathologic examination. Fixed bones were decalcified overnight in Cal-EX (Fisher Diagnostics) solution containing 0.03 mol/L chelating agent sodium-EDTA and 1.35 N HCl, and then washed in running water for 3 to 4 h followed by conventional processing for sectioning. In each case, 5-μm-thick sections of paraffin-embedded tissues were stained with H&E for histopathologic evaluation.

***Immunohistochemical analysis.*** Paraffin-embedded tissue sections were deparaffinized and stained using specific primary antibody followed by 3,3-diaminobenzidine staining, as previously described (21). Primary antibodies used were anti–proliferation cell nuclear antigen (1:250 dilution; Dako), goat polyclonal anti-CD31 (1:200 dilution; Santa Cruz Biotechnology, Inc.), and rabbit polyclonal anti-VEGF (1:100 dilution, Santa Cruz Biotechnology). Biotinylated secondary antibodies used were rabbit anti-mouse IgG (1:200; Dako) and goat anti-rabbit IgG (1:200; Santa Cruz Biotechnology). Apoptotic cells were identified by terminal deoxynucleotidyl transferase-mediated dUTP nick end labeling (TUNEL) staining using Dead End Colorometric TUNEL System (Promega Corp.) as published (17, 18). Proliferating cell nuclear antigen– and TUNEL-positive cells were quantified by counting

Downloaded from http://aacrjournals.org/clincancerres/article-pdf/14/23/7773/1979631/7773.pdf by guest on 03 March 2024

brown-stained cells within the total number of cells at 10 randomly selected fields at ×400 magnification. Tumor microvessel density was quantified by counting the CD31-positive cells at 10 randomly selected fields at ×400 magnification. Branching vessels (i.e., a group of CD31-positive cells connected with each other) were considered as one count. For VEGF, immunoreactivity (represented by intensity of brown staining) was scored as 0 (no staining), +1 (nonuniform and very weak), +2 (nonuniform and weak), +3 (uniform and moderate), and +4 (uniform and strong) as reported (21). In all immunohistochemical staining, negative staining controls (and positive staining control for TUNEL by incubation with nuclease to generate nicks) were used, where sections were incubated with N-Universal Negative Control-mouse or rabbit antibody (Dako) under identical conditions.

***Western immunoblot analysis.*** Dorsolateral prostate samples from control and silibinin-fed groups of mice were analyzed by immunoblotting as previously described (19). Randomly, three tumors were selected from each group (control, 0.5% and 1% silibinin groups) and homogenized in nondenaturing lysis buffer and centrifuged at 14,000 × *g* followed by protein concentration determination in supernatants. Equal protein per lysate was resolved on Tris-glycine gel, transferred onto nitrocellulose membrane, and blocked for 1 h with 5% nonfat dry milk. Membranes were incubated with specific primary antibodies including anti-VEGF, anti–VEGF-R2, anti–MMP-3, anti–E-cadherin, and anti-vimentin from Santa Cruz Biotechnology; anti–MMP-2 from Chemicon International; and anti–snail-1 from Abcam, overnight at 4°C and then with appropriate horseradish peroxidase–conjugated secondary antibody followed by ECL detection. Blots were scanned with Adobe Photoshop 6.0 with minimum background. Densitometric analysis was done with Scion image software (NIH) and data are shown as fold change of the control value. Membranes were stripped and reprobed with anti–β-actin antibody for loading control.

***Mouse angiogenesis antibody array.*** Plasma samples collected at the end of the experiment after 11 wk of silibinin treatment were used to analyze the levels of circulating angiogenesis-related molecules using a Mouse Angiogenesis Antibody Array (RayBiotech, Inc.) as recently reported by us (21). A representative plasma sample (100 μL/assay) from control and 1% silibinin-treated groups was analyzed according to the manufacturer's assay protocol. Each protein expression was represented by a pair of dots (duplex dots) on the membrane. Duplex dots identifying each protein were scanned by Photoshop Adobe and quantitated by ScionImage program (NIH). The mean value of the intensity of the two dots in arbitrary unit was determined for intergroup comparison.

***Statistical and microscopic analyses.*** All statistical analyses were carried out with Sigma Stat software version 2.03 (Jandel Scientific) and *P* values <0.05 were considered significant. Fisher's exact test was used to compare incidence of prostatic intraepithelial neoplasia (PIN), adenocarcinoma, invasion of seminal vesicle, and metastatic lesions in (31-wk) control versus other groups. For other data, the difference between control and silibinin-fed groups was analyzed by Student's *t* test. All microscopic histopathologic and immunohistochemical analyses were done by Zeiss Axioscope 2 microscope (Carl Zeiss, Inc.) and photomicrographs were captured by Carl Zeiss AxioCam MrC5 camera and shown at ×400 magnification.

## Results

***Silibinin inhibits palpable prostate tumor growth in TRAMP mice.*** TRAMP male mice at 20 weeks of age, each having palpable prostate tumor, were fed with purified AIN-93M diet (control) or the diet containing 0.5% or 1%, w/w, silibinin (Fig. 1B). The efficacy of the treatment was measured weekly by the absence or presence of a palpable tumor, until 31 weeks of the age, which indicated slower increase in tumor mass in mice fed with silibinin diets compared with control. Animal health, body weight, and diet consumption were also monitored

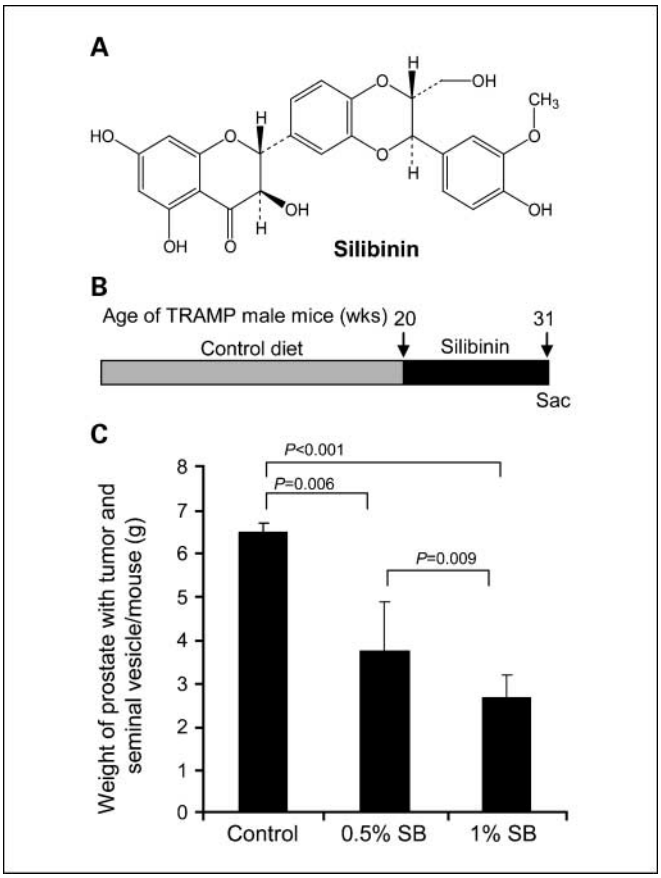


**Fig. 1.** Inhibition of established prostate tumor growth by dietary silibinin in TRAMP mice. *A,* chemical structure of the flavanolignan compound silibinin. *B,* experimental design in which 20-wk-old TRAMP male mice were sacrificed or exposed to AIN-93M control diet or control diet containing 0.5% and 1% (w/w) silibinin for 11 wk. *C,* cumulative weight of en bloc prostate with tumor and seminal vesicle (g) per mouse at the termination of the experiment (31 wk of age). Columns, mean from 7 to 8 mice in each group; bars, SE. Sac, sacrificed; SB, silibinin.

biweekly, which did not show any change due to silibinin supplementation in diet (data not shown). At 31 weeks of age, silibinin diets significantly and dose-dependently decreased (up to 60%) the weight of prostate together with tumor and seminal vesicle, which were 3.7 ± 0.5 g/mouse ($P < 0.006$) and 2.6 ± 0.8 g/mouse ($P < 0.001$) in the lower and higher doses of silibinin groups compared with 6.5 ± 1.2 g/mouse in control group, respectively (Fig. 1C). The corresponding weight of prostate with seminal vesicle in 31-week-old wild-type mice fed with control diet was 2.0 ± 0.2 g/mouse that did not show any considerable change due to 11 weeks of 1% silibinin consumption in diet (data not shown). These observations suggest that silibinin feeding at these doses is nontoxic and that it selectively as well as dose-dependently suppresses the aberrant or neoplastic growth of prostate tissue. It is likely that silibinin, in addition to inhibition, may also cause the reversal of the disease progression in this animal model. This is supported by the earlier studies in which approximately more than half of TRAMP mice at 20 weeks of age have shown the different stages of adenocarcinoma (22). Next, prostate tissue samples were analyzed for histopathologic alterations.

***Silibinin inhibits the progression of established prostate tumor in TRAMP mice.*** H&E-stained tissue sections were microscopically examined for the presence of PIN showing the

Downloaded from http://aacrjournals.org/clincancerres/article-pdf/14/23/7773/1979631/7773.pdf by guest on 03 March 2024

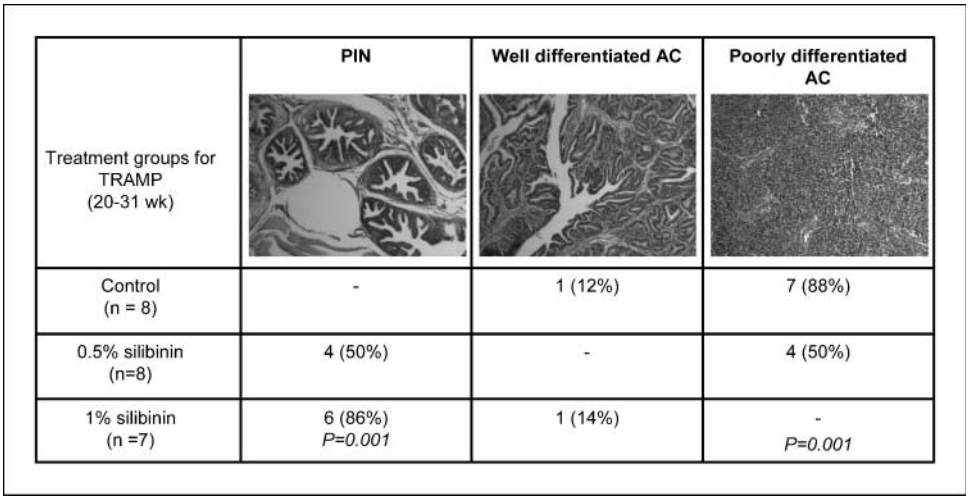


**Fig. 2.** Inhibition of tumor progression by dietary silibinin in TRAMP mice with established prostate tumors. The prostate tissue samples from the experiment detailed in Fig. 1 were histopathologically analyzed for various stages of prostate tumor progression, including PIN, well-differentiated adenocarcinoma, and poorly differentiated adenocarcinoma as described in Materials and Methods. The incidence of each stage is shown from 7 to 8 mice in each group, and values in parentheses indicate percent incidence for that group. Fisher's exact test was done to compare control group with silibinin-treated groups for each stage of prostate cancer.

characteristics of foci with two or more layers of atypical cells, with elongated hyperchromatic nuclei filling or almost filling the lumen of the ducts with distorted duct and cribriform structures, and intact or enlarged gland profiles; well-differentiated adenocarcinoma showing invasion of basement membrane, loss of intraductal spaces, and increased quantity of small glands; and poorly differentiated adenocarcinoma showing total loss of intraductal spaces and the presence of poorly differentiated cells with leftovers of trapped glands with fairly solid growth (19, 23). Histopathologic analysis of prostate showed a marked difference for the incidence of PIN, well-differentiated adenocarcinoma, and poorly differentiated adenocarcinoma between the 31-week control and both silibinin-treated groups. Also, the portions of the prostate with these progressive neoplastic stages were decreased by silibinin treatments. At 31 weeks of age, there was a complete absence of PIN with 12% and 88% incidences of well-differentiated adenocarcinoma and poorly differentiated adenocarcinoma, respectively, in control mice (Fig. 2). Silibinin treatments at 0.5% and 1% doses inhibited the progression of PIN into the advanced stages of prostate cancer by 50% and 86% ($P$ = 0.001), respectively. More importantly, silibinin also suppressed the severity of adenocarcinoma with the increase in its doses, showing 50% incidence of poorly differentiated adenocarcinoma at 0.5% silibinin dose, which was completely absent at 1% silibinin dose that showed only 14% incidence for well-differentiated adenocarcinoma (Fig. 2). In age-matched nontransgenic mice at 31 weeks, no difference was observed in the prostate histopathology between the control and silibinin-treated groups (data not shown). These results suggest that the introduction of silibinin treatment to TRAMP mice bearing tumor was dose-dependently effective in arresting the tumor progression at the PIN stage and thereby reduce the incidence of adenocarcinoma. Further, silibinin also decreased the aggressiveness and severity of adenocarcinoma.

***Silibinin inhibits tumor invasion and metastasis in TRAMP mice.*** During the tumor progression in TRAMP, prostate tumor can invade surrounding tissues such as seminal vesicle; at advanced stages, it metastasizes to the distant organs. At necropsy, in the 31-week control group, 6 of 8 (75%) mice had invasive tumor showing local invasion of seminal vesicles (Table 1). In lower and higher doses of silibinin groups, 4 of 8 (50%) and 1 of 7 (14%, $P$ = 0.04 versus 31-week control) mice had the incidence of prostate tumor invasion of seminal vesicles, respectively, all of which were confirmed by histopathology (Table 1). A phenomenal antimetastatic effect of silibinin was also observed with no secondary tumors in distant organs (including liver, kidney, lung, lymph node, and bone), whereas the 31-week control group showed three cases of metastatic lesions, two in liver and one in kidney, in which one mouse had lesions in both liver and kidney (Table 1). These findings suggest the anti-invasive and antimetastatic effects of silibinin during prostate cancer progression.

***Silibinin inhibits cell proliferation, survival, and angiogenesis in established prostate tumor in TRAMP mice.*** The immunohistochemical analysis of prostate tumors showed inhibition of

**Table 1.** Inhibitory effect of silibinin on prostate tumor invasion of seminal vesicle and distant metastasis in TRAMP mice

| Treatment groups for TRAMP (20-31 wk) | Tumor invasion of seminal vesicle | Secondary tumor in liver | Secondary tumor in kidney |
|---|---|---|---|
| Control ($n$ = 8) | 6 (75%) | 2 (25%) | 1 (12%) |
| 0.5% Silibinin ($n$ = 8) | 4 (50%) | | |
| 1.0% Silibinin ($n$ = 7) | 1 (14%), $P$ = 0.04 | | |

NOTE: The incidence of tumor invasion of seminal vesicle and distant metastasis in liver and kidney are from the study detailed in Fig. 1, with each group having 7 to 8 mice. Values in parentheses show percent incidence for that group. Fisher's exact test was done to compare control group with silibinin-treated groups for each event of prostate cancer development.

Downloaded from http://aacrjournals.org/clincancerres/article-pdf/14/23/7773/1979631/7773.pdf by guest on 03 March 2024

cell proliferation (up to 40%, $P = 0.015$) and an induction of apoptosis (up to 2-fold, $P = 0.006$) by silibinin (data not shown), which is consistent with its similar effects in other tumor models, including prostate cancer (17–20). During prostate cancer progression, the intraductal microvessel density increases as a function of tumor grade with the transition from PIN to differentiated and poorly differentiated adenocarcinoma stages, which has been observed in clinical prostate cancer specimens (24, 25). TRAMP mice on control diet for 11 weeks showed prostate tumors with enriched vasculature (Fig. 3A, *left*), which was strongly reduced by silibinin diets (Fig. 3A, *right*). The quantification of microvessel density showed $12 \pm 1$ ($P < 0.01$) and $8 \pm 2$ ($P < 0.001$) microvessels (CD31-positive cells) per field in lower and higher doses of silibinin groups compared with $20 \pm 2$ in control group, respectively, which accounts for 40% to 60% decrease in tumor microvessel density (Fig. 3B). These results suggest that the antiangiogenic effect of silibinin, together with antiproliferative and proapoptotic activities, possibly plays a major role in its inhibitory potential on prostate cancer growth and progression. We further explored the potential molecular antiangiogenic targets of silibinin in tumors and circulating mouse plasma.

***Silibinin suppresses the levels of angiogenic growth factors and receptor.*** Immunohistochemical analysis of tumors showed decreased levels of VEGF immunoreactivity in the silibinin-treated group compared with the control group (Fig. 3A, *bottom*), which was evident in quantitative data for the same (Fig. 3C). These results were confirmed by immunoblot analysis of tumor samples that showed a marked dose-dependent decrease in the expression levels of VEGF as well as VEGFR-2 by silibinin (Fig. 4A). Further, we did an angiogenic cytokine array in mouse plasma from control and 1% silibinin-treated groups and found that silibinin strikingly decreases circulating levels of basic fibroblast growth factor (bFGF) by 64% and VEGF by 43% compared with that of the control group (Fig. 3D). These results indicated the predominant antiangiogenic effect of silibinin as a potential mechanism to suppress prostate tumor growth, progression, and metastasis. Another important observation was made in this study where ~3-fold higher levels of bFGF were noted when compared with the level of VEGF at the 31-week age of TRAMP mice, which was associated with the advanced and metastatic disease phenotypes.

***Silibinin suppresses molecular events driving invasion and epithelial-mesenchymal-transition in prostate tumor.*** Further, we examined the potential molecular targets of silibinin for its anti-invasive and antimetastatic activities. At the end of 11 weeks of treatment, three tumor samples from each group were randomly selected for the Western immunoblot analysis. As MMPs degrade tissue matrix and facilitate tumor invasion,

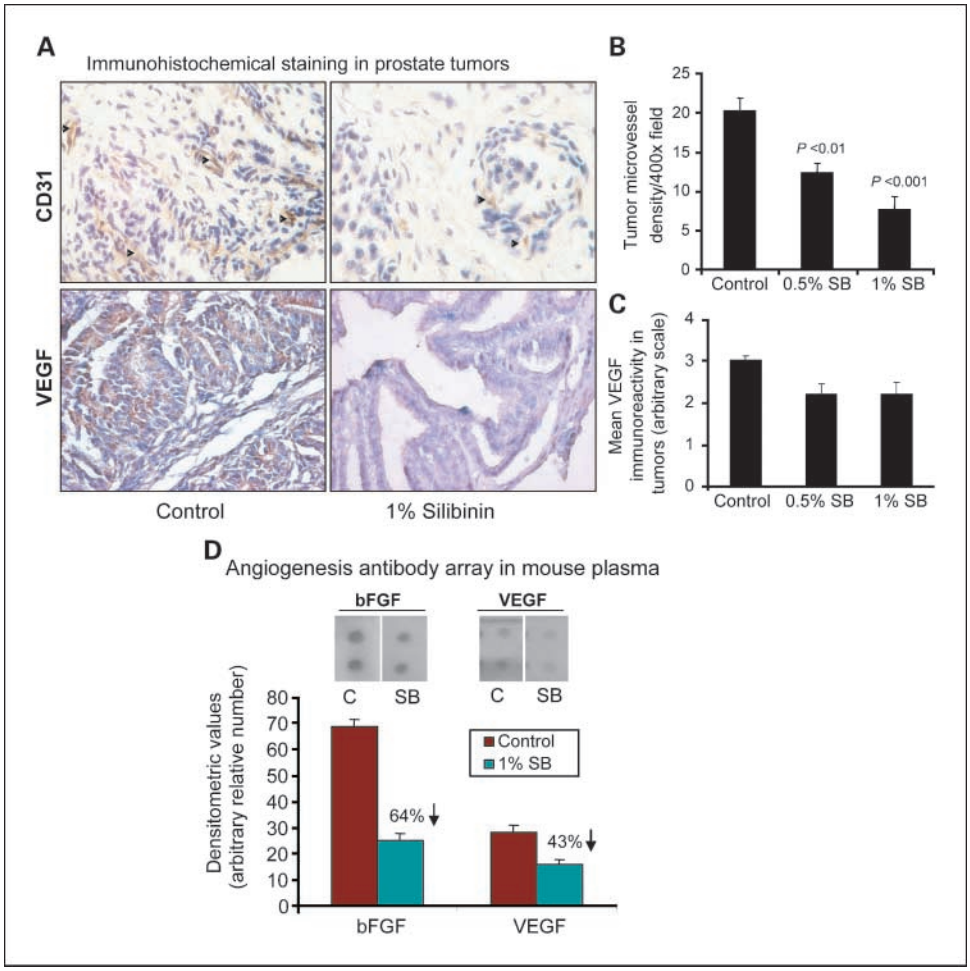


**Fig. 3.** Inhibitory effect of silibinin on tumor angiogenesis in TRAMP mice with established prostate tumors. *A,* prostate tissue samples from the experiment detailed in Fig. 1 (at 31 wk of mice age) were immunohistochemically analyzed for CD31-positive microvessels and VEGF immunoreactivity as detailed in Materials and Methods. The representative pictograph (×400) for CD31-positive brown-stained endothelial cells (*arrowheads*) and VEGF expression (*brown*) are shown from control and 1% silibinin-treated groups. Quantitative data for (*B*) microvessel density per ×400 microscopic field and (*C*) levels of VEGF expression in prostate tumor are shown from 7 to 8 mice in each group. Columns, mean; bars, SE. *D,* a representative plasma sample each from control and 1% silibinin-treated groups was analyzed by angiogenic cytokine array for the circulating levels of angiogenic factors as detailed in Materials and Methods. The marked inhibitory effect of silibinin was observed for bFGF and VEGF. The array was quantified by densitometry. Columns, mean of duplicate dots for each molecule shown in the figure; bars, SE. *C,* control (31 wk). CD31, cluster of differentiation 31 and endothelial cell marker.

Downloaded from http://aacrjournals.org/clincancerres/article-pdf/14/23/7773/1979631/7773.pdf by guest on 03 March 2024

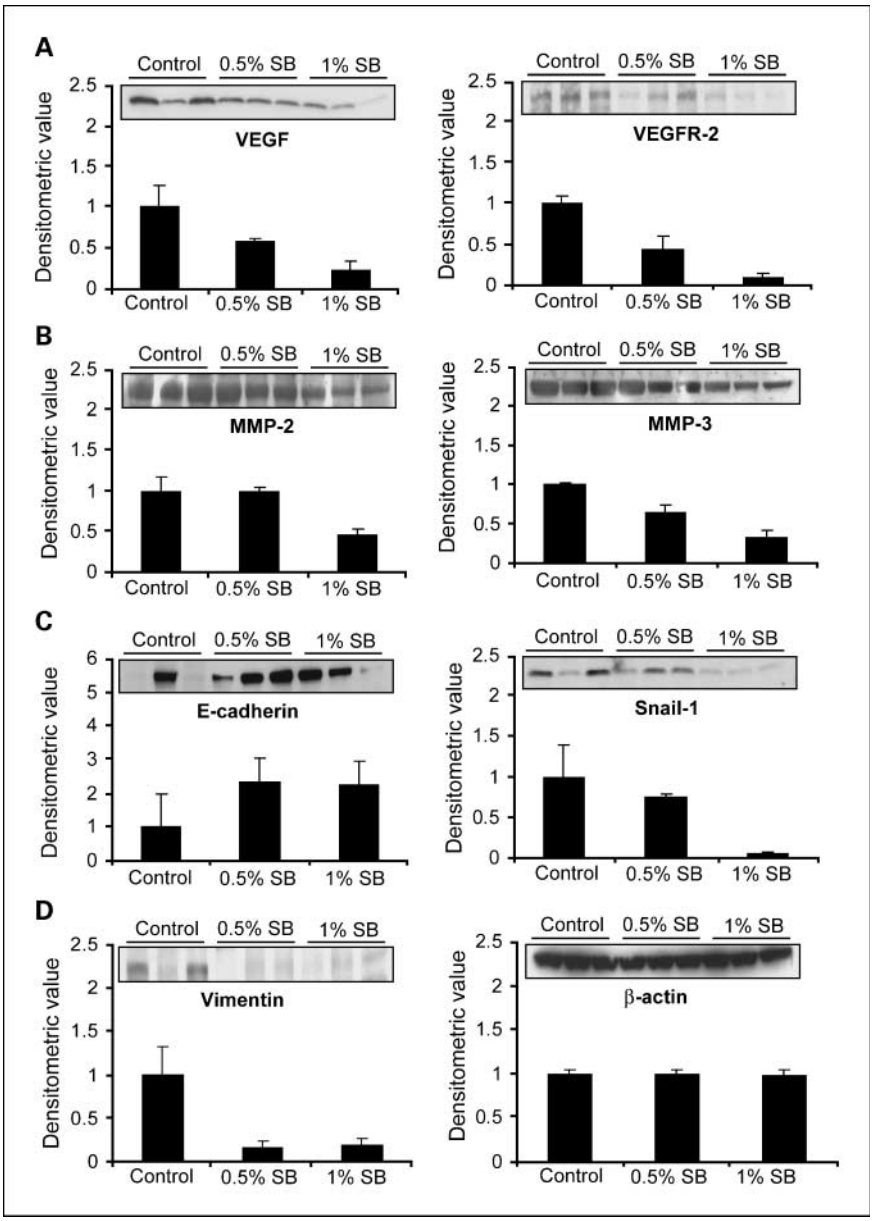


**Fig. 4.** Effect of silibinin on molecular events related to angiogenesis, invasion, and EMT in established prostate tumor in TRAMP mice. At the end of the experiment (31 wk of mice age), three tumors were randomly selected from each of control and 0.5% and 1% silibinin-treated groups, and analyzed by Western immunoblotting for the molecules related to angiogenesis, invasion, and metastasis. A marked decrease in expression of (*A*) VEGF, VEGFR-2; (*B*) MMP-2, MMP-3; (*C, left*) snail-1 and (*D, left*) vimentin; and (*C, right*) an increase in E-cadherin expression were noted. Membranes were stripped and reprobed for (*D, right*) β-actin as loading control; a representative blot is shown. In each case, densitometric analysis of the bands were carried out. Columns, mean from three samples for each group below the blot; bars, SE.

we first analyzed their levels wherein MMP-2 ($P < 0.05$) and MMP-3 ($P < 0.01$) levels were decreased in tumors by silibinin treatments, specifically at higher doses (Fig. 4B). The loss of E-cadherin and the corresponding increase in vimentin causes EMT, which is a critical stage in invasion and migration of tumor cells of epithelial origin (10). Snail-1 is known as master regulator of EMT as well as a transcriptional repressor of E-cadherin (11). Silibinin treatments showed increased level of E-cadherin in parallel with a decrease in vimentin and also decreased level of snail-1 in tumors (Fig. 4C-D). All the blots were subjected to densitometric analysis of the bands, which was adjusted with the level of β-actin that did not show any change for all the samples (Fig. 4D). These results suggest that silibinin could target the expression of MMP as well as EMT via snail-1–mediated regulation of E-cadherin and vimentin for its anti-invasive and antimetastatic activities in prostate cancer.

## Discussion

The genetically engineered mouse models of cancer have widely been used to understand the mechanisms of multistage carcinogenesis in the tissue microenvironment. The TRAMP model closely mimics human prostate growth and progression and provides an excellent opportunity for the intervention studies (26–28). In this model, androgen-regulated and probasin-driven expression of SV40 large T antigen abrogates p53 and Rb function to spontaneously develop the progressive stages of prostate cancer from PIN to the advanced stages of adenocarcinoma that subsequently leads to metastatic dissemination of tumor cells to distant organs (22, 28–30). Although in humans, prostate cancer is mostly diagnosed at advanced stages, efforts are being made for its early detection through screening for different biomarkers. There could be a clinical situation in which prostate tumor is diagnosed at the PIN stage to provide

Downloaded from http://aacrjournals.org/clincancerres/article-pdf/14/23/7773/1979631/7773.pdf by guest on 03 March 2024

enough time to decide for the treatment options. In the present preclinical intervention study, all mice had palpable tumor when the silibinin treatment started. Therefore, our present findings of antitumor efficacy of silibinin in TRAMP mice with established tumors could have potential clinical significance.

The antitumor effect of silibinin on established prostate tumor was observed in terms of (*a*) reduction of tumor mass, (*b*) inhibition of tumor progression from PIN stage with a concomitant decrease in the incidence of adenocarcinoma, (*c*) reduced severity of adenocarcinoma (i.e., well-differentiated versus poorly differentiated adenocarcinoma), (*d*) decreased incidence of tumor invasion of seminal vesicle, and (*e*) reduced incidence of distant metastasis. These effects were mostly silibinin dose dependent. We have recently reported that TRAMP mice fed with silibinin diets for 20 weeks, starting at 4 weeks of age where these mice have normal prostatic epithelium (as tumor initiation is hormonally regulated and starts when mice reach at puberty), show suppression of prostate tumor progression with moderate effect on the tumor mass (19). In the present study with established tumor, silibinin suppressed the growth of tumor mass as well as inhibited tumor progression from PIN to the advanced adenocarcinoma stages. Silibinin (at 1% dose) showed absolute absence of poorly differentiated adenocarcinoma whereas 88% of control mice showed this stage of prostate cancer. These findings suggest that in addition to its efficacy at early stages of prostate cancer development (19), silibinin could be useful for the intervention of prostate cancer diagnosed at relatively advanced stages. This suggestion is also supported by the fact that silibinin inhibits the growth of human prostate carcinoma DU145 and PC3 tumor xenografts in athymic nude mice model (17, 18).

While exploring the biomarkers of antitumor effects of silibinin in the present study, we observed moderate effects of silibinin in inhibiting tumor cell proliferation and apoptosis induction. At the molecular level, silibinin could target the IGF-I–IGFBP-3 axis and the CDK-cyclin-CDKI and EGF receptor signaling to inhibit cell proliferation, and activate the caspase pathway to induce apoptosis as observed in different studies (4, 17–19). Our next focus was to examine its antiangiogenic effect as we observed its strong inhibitory effects on tumor growth as well as progression, invasion, and metastasis. There are studies that establish the potential role as well as diagnostic and prognostic values of angiogenesis in prostate cancer progression and metastasis (24, 31, 32). Silibinin has shown its direct inhibitory effect on endothelial cell proliferation, survival, migration, and capillary organization in cell culture (33). Immunohistochemical analysis of tumors for microvessels showed a significant dose-dependent decrease in microvessel density by silibinin, which was accompanied by the decrease in VEGF expression. Because circulating levels of angiogenic factor could also relate with the angiogenic stage of the tumor, an array analysis was done for the same in mouse plasma. Two significant observations were made in which, first, the control mouse having advanced prostate cancer showed higher levels of bFGF compared with VEGF, and, second, the levels of both these endothelial cell mitogens were strongly decreased by silibinin treatment. VEGFR-2, also known as kinase insert domain-containing receptor/fetal liver kinase-1 (KDR/Flk1), is constitutively expressed in endothelial cells and also expressed in tumor cells, and mediates endothelial cell proliferation, differentiation and survival, and modulation of developmental angiogenesis through the interaction with VEGF (34, 35). VEGF binding with VEGFR-2 causes its dimerization and oligomerization, which activates its intrinsic tyrosine kinase activity resulting in activation of downstream signaling cascades for different biological effects (35, 36). Therefore, we also analyzed the tumor level of VEGFR-2, which was decreased by silibinin treatment similar to its inhibitory effect on VEGF. These findings suggest that silibinin, in addition to lowering the level of bFGF, potentially targets the VEGF-VEFGR-2 axis for its antiangiogenic effect in prostate tumors.

Furthermore, we investigated the anti-invasive and antimetastatic activities of silibinin in an *in vivo* tumor model. Dietary silibinin showed an inhibition of invasiveness of growing prostate tumors to the seminal vesicle. In the control mice, gross observation showed that most parts of the seminal vesicles were encroached by tumor tissues. Additionally, most of them were also reddish in color, indicating the higher level of blood circulation. Such appearances of tumor growth in adjacent seminal vesicle indicated the coupling of invasion with angiogenesis in which the latter can facilitate the former for the expansion of tumor mass. Moreover, angiogenesis and invasion potentially lead to metastatic spread of cancer cells (29–31). At the termination of the experiment, three cases of metastatic lesions were observed in distant organs in control mice, which were completely absent in silibinin-treated mice. While analyzing the mechanistic events underlying the invasive and metastatic potential of these prostate tumors and their modulation by silibinin, we observed the higher levels of MMP-2 and MMP-3 in the control group, which were decreased by silibinin (at higher dose). The mechanisms by which silibinin decreases the levels of MMPs and VEGFR-2 are yet to be investigated; however, we anticipate that inhibition of mitogenic and angiogenic signaling by silibinin could mediate these effects.

Recently, EMT has been observed to play a critical role in invasion and metastasis of epithelial tumors (10, 11). This process is mainly coordinated by the disappearance of E-cadherin with the concomitant appearance of vimentin (11, 37, 38). Loss of E-cadherin function or expression is implicated in cancer progression and metastasis, which leads to decreased strength of cellular adhesion within the tissue, resulting in an increase in cellular motility and invasiveness (37). Subsequently, this could allow cancer cells to cross the basement membrane and invade surrounding tissues as observed in the present study, in which 75% of control mice showed tumor invasion of seminal vesicle. Snail-1 is a transcription factor that is known to transcriptionally repress E-cadherin during the process of EMT (11, 39). Snail-1 can also target MMP for up-regulation in tumors (40). In the present study, silibinin treatment showed the reappearance of E-cadherin with a concomitant strong decrease in the level of vimentin. As anticipated, silibinin also decreased the level of snail-1, suggesting a possible transcriptional up-regulation of E-cadherin and a concomitant down-regulation of vimentin by silibinin. Overall, these findings showed that silibinin may target the E-cadherin–vimentin equilibrium via down-regulation of snail-1 to inhibit EMT and consequently suppress invasion and metastasis of prostate tumor.

In summary, these findings suggest that the moderate antiproliferative and proapoptotic effects of silibinin together

Downloaded from http://aacrjournals.org/clincancerres/article-pdf/14/23/7773/1979631/7773.pdf by guest on 03 March 2024

with its strong antiangiogenic and anti-EMT effects could inhibit prostate tumor growth, progression, invasion, and metastasis. The antiangiogenic effect of silibinin could involve the down-regulation of VEGF, VEGFR-2, and bFGF, whereas its anti-EMT effect could be mediated by modulating MMP, E-cadherin, and vimentin through snail-1. These findings could have clinical relevance to control human prostate cancer. In this regard, we have recently completed a phase I clinical trial with silibinin in prostate cancer patients (41); moreover, a phase II clinical trial is ongoing where present findings may find a vital practical and greater translational relevance.

## Disclosure of Potential Conflicts of Interest

No potential conflicts of interest were disclosed.

## References


1. Stoner GD, Wang LS, Zikri N, et al. Cancer prevention with freeze-dried berries and berry components. Semin Cancer Biol 2007;17:403–10.
2. Singh RP, Agarwal R. Mechanisms of action of novel agents for prostate cancer chemoprevention. Endocr Relat Cancer 2006;13:751–78.
3. Wellington K, Jarvis B. Silymarin: a review of its clinical properties in the management of hepatic disorders. BioDrugs 2001;15:465–89.
4. Singh RP, Agarwal R. Prostate cancer chemoprevention by silibinin: bench to bedside. Mol Carcinog 2006;45:436–42.
5. Joshua AM, Evans A, Van der Kwast T, et al. Prostatic preneoplasia and beyond. Biochim Biophys Acta 2008;1785:156–81.
6. Jemal A, Siegel R, Ward E, Murray T, Xu J, Thun MJ. Cancer Statistics, 2007. CA Cancer J Clin 2007;57:43–66.
7. Hadaschik BA, Gleave ME. Therapeutic options for hormone-refractory prostate cancer in 2007. Urol Oncol 2007;25:413–9.
8. Neri D, Bicknell R. Tumour vascular targeting. Nat Rev Cancer 2005;5:436–46.
9. Overall CM, Kleifeld O. Tumour microenvironment—opinion: validating matrix metalloproteinases as drug targets and anti-targets for cancer therapy. Nat Rev Cancer 2006;6:227–39.
10. Thiery JP. Epithelial-mesenchymal transitions in tumour progression. Nat Rev Cancer 2002;2:442–54.
11. Thiery JP, Sleeman JP. Complex networks orchestrate epithelial-mesenchymal transitions. Nat Rev Mol Cell Biol 2006;7:131–42.
12. Zi X, Agarwal R. Silibinin decreases prostate-specific antigen with cell growth inhibition via G1 arrest, leading to differentiation of prostate carcinoma cells: implications for prostate cancer intervention. Proc Natl Acad Sci U S A 1999;96:7490–5.
13. Deep G, Singh RP, Agarwal C, Kroll DJ, Agarwal R. Silymarin and silibinin cause $G_1$ and $G_2$-M cell cycle arrest via distinct circuitries in human prostate cancer PC3 cells: a comparison of flavanone silibinin with flavanolignan mixture silymarin. Oncogene 2006;25:1053–69.
14. Tyagi A, Agarwal C, Agarwal R. Inhibition of retinoblastoma protein (Rb) phosphorylation at serine sites and an increase in Rb-E2F complex formation by silibinin in androgen-dependent human prostate carcinoma LNCaP cells: role in prostate cancer prevention. Mol Cancer Ther 2002;1:525–32.
15. Zi X, Grasso AW, Kung HJ, Agarwal R. A flavonoid antioxidant, silymarin, inhibits activation of erbB1 signaling and induces cyclin-dependent kinase inhibitors, G1 arrest, and anticarcinogenic effects in human prostate carcinoma DU145 cells. Cancer Res 1998;58:1920–9.
16. Zi X, Zhang J, Agarwal R, Pollak M. Silibinin up-regulates insulin-like growth factor-binding protein 3 expression and inhibits proliferation of androgen-independent prostate cancer cells. Cancer Res 2000;60:5617–20.
17. Singh RP, Dhanalakshmi S, Tyagi AK, Chan DC, Agarwal C, Agarwal R. Dietary feeding of silibinin inhibits advance human prostate carcinoma growth in athymic nude mice and increases plasma insulin-like growth factor-binding protein-3 levels. Cancer Res 2002;62:3063–9.
18. Singh RP, Deep G, Blouin MJ, Pollak MN, Agarwal R. Silibinin suppresses *in vivo* growth of human prostate carcinoma PC-3 tumor xenograft. Carcinogenesis 2007;28:2567–74.
19. Raina K, Blouin MJ, Singh RP, et al. Dietary feeding of silibinin inhibits prostate tumor growth and progression in transgenic adenocarcinoma of the mouse prostate model. Cancer Res 2007;67:11083–91.
20. Singh RP, Gu M, Agarwal R. Silibinin inhibits colorectal cancer growth by inhibiting tumor cell proliferation and angiogenesis. Cancer Res 2008;68:2043–50.
21. Singh RP, Deep G, Chittezhath M, et al. Effect of silibinin on the growth and progression of primary lung tumors in mice. J Natl Cancer Inst 2006;98:846–55.
22. Kaplan-Lefko PJ, Chen TM, Ittmann MM, et al. Pathobiology of autochthonous prostate cancer in a pre-clinical transgenic mouse model. Prostate 2003;55:219–37.
23. Shappell SB, Thomas GV, Roberts RL, et al. Prostate pathology of genetically engineered mice: definitions and classification. The consensus report from the Bar Harbor meeting of the Mouse Models of Human Cancer Consortium Prostate Pathology Committee. Cancer Res 2004;64:2270–305.
24. Hrouda D, Nicol DL, Gardiner RA. The role of angiogenesis in prostate development and the pathogenesis of prostate cancer. Urol Res 2003;30:347–55.
25. Bostwick DG, Aquilina JW. Prostatic intraepithelial neoplasia (PIN) and other prostatic lesions as risk factors and surrogate endpoints for cancer chemoprevention trials. J Cell Biochem Suppl 1996;25:156–64.
26. Gingrich JR, Greenberg NM. A transgenic mouse prostate cancer model. Toxicol Pathol 1996;24:502–4.
27. Gingrich JR, Barrios RJ, Kattan MW, Nahm HS, Finegold MJ, Greenberg NM. Androgen-independent prostate cancer progression in the TRAMP model. Cancer Res 1997;57:4687–91.
28. Greenberg NM, DeMayo FJ, Sheppard PC, et al. The rat probasin gene promoter directs hormonally and developmentally regulated expression of a heterologous gene specifically to the prostate in transgenic mice. Mol Endocrinol 1994;8:230–9.
29. Gingrich JR, Barrios RJ, Foster BA, Greenberg NM. Pathologic progression of autochthonous prostate cancer in the TRAMP model. Prostate Cancer Prostatic Dis 1999;2:70–5.
30. Gingrich JR, Barrios RJ, Morton RA, et al. Metastatic prostate cancer in a transgenic mouse. Cancer Res 1996;56:4096–102.
31. Huss WJ, Hanrahan CF, Barrios RJ, Simons JW, Greenberg NM. Angiogenesis and prostate cancer: identification of a molecular progression switch. Cancer Res 2001;61:2736–43.
32. Isayeva T, Chanda D, Kallman L, Eltoum IE, Ponnazhagan S. Effects of sustained antiangiogenic therapy in multistage prostate cancer in TRAMP model. Cancer Res 2007;67:5789–97.
33. Singh RP, Dhanalakshmi S, Agarwal C, Agarwal R. Silibinin strongly inhibits growth and survival of human endothelial cells via cell cycle arrest and downregulation of survivin, Akt and NF-κB: implications for angioprevention and antiangiogenic therapy. Oncogene 2005;24:1188–202.
34. Khosravi Shahi P, Fernández Pineda I. Tumoral angiogenesis: review of the literature. Cancer Invest 2008;26:104–8.
35. Shibuya M. Vascular endothelial growth factor (VEGF)-receptor2: its biological functions, major signaling pathway, and specific ligand VEGF-E. Endothelium 2006;13:63–9.
36. Olsson AK, Dimberg A, Kreuger J, Claesson-Welsh L. VEGF receptor signalling—in control of vascular function. Nat Rev Mol Cell Biol 2006;7:359–71.
37. Frixen UH, Behrens J, Sachs M, et al. E-cadherin-mediated cell-cell adhesion prevents invasiveness of human carcinoma cells. J Cell Biol 1991;113:173–85.
38. Lang SH, Hyde C, Reid IN, et al. Enhanced expression of vimentin in motile prostate cell lines and in poorly differentiated and metastatic prostate carcinoma. Prostate 2002;52:253–63.
39. Batlle E, Sancho E, Francí C, et al. The transcription factor snail is a repressor of E-cadherin gene expression in epithelial tumour cells. Nat Cell Biol 2000;2:84–9.
40. Peinado H, Olmeda D, Cano A. Snail, Zeb and bHLH factors in tumour progression: an alliance against the epithelial phenotype? Nat Rev Cancer 2007;7:415–28.
41. Flaig TW, Gustafson DL, Su LJ, et al. A phase I and pharmacokinetic study of silybin-phytosome in prostate cancer patients. Invest New Drugs 2007;25:139–46.


Downloaded from http://aacrjournals.org/clincancerres/article-pdf/14/23/7773/1979631/7773.pdf by guest on 03 March 2024